Cigarette smoke induces overexpression of active human cathepsin S in lungs from current smokers with or without COPD

Pierre-Marie Andrault[1,2,#,*], Andrea C. Schamberger[3*], Thibault Chazeirat[1,2], Damien Sizaret[1,4], Justine Renault[1, †], Claudia A. Staab-Weijnitz[3], Elisabeth Hennen[3], Agnès Petit-Courty[1,2], Mylène Wartenberg[1,2], Ahlame Saidi[1,2], Thomas Baranek[1,2], Serge Guyetant[1,4], Yves Courty[1,2], Oliver Eickelberg[3, ‡], Gilles Lalmanach[1,2], Fabien Lecaille[1,2¶]

[1] Université de Tours, Tours, France
[2] INSERM, UMR 1100, Centre d'Etude des Pathologies Respiratoires, Team Mécanismes Protéolytiques dans l'Inflammation, Tours, France.
[3] Comprehensive Pneumology Center, Institute of Lung Biology and Disease, University Hospital, Ludwig-Maximilians-University and Helmholtz Zentrum München, Member of the German Center for Lung Research (DZL), Munich, Germany.
[4] Centre Hospitalier Régional Universitaire de Tours (CHRU Tours), Service d'Anatomie et Cytologie Pathologique, Tours, France.

[#] Current address: Department of Oral Biological and Medical Sciences, Faculty of Dentistry, University of British Columbia, Vancouver, Canada.
[†] Current address: Unité de Biologie Fonctionnelle et Adaptative, CNRS, UMR 8251, Université Paris Diderot, Paris 7, France
[‡] Current address: Division of Pulmonary and Critical Care Medicine, University of Colorado Anschutz School of Medicine, Aurora, USA.

[¶]Corresponding author information : Fabien Lecaille, PhD, Université de Tours, INSERM, UMR 1100, CEPR, 10 Boulevard Tonnellé, F-37032 Tours cedex, France. Tel: (+33) 247366047; e-mail: fabien.lecaille@univ-tours.fr

*These authors contributed equally to this manuscript.

Running title: Cigarette smoke increases human cathepsin S activity

Abbreviations:

AEBSF, 4-(2-aminoethyl) benzenesulfonyl fluoride hydrochloride; AMP, antimicrobial peptide and protein; ASL, airway surface liquid ; BALF, bronchoalveolar lavage fluid ; BM, basement membrane; CA-074, N-(L-3-trans-propylcarbamoyloxirane-2-carbonyl)-L-isoleucyl-L-proline; Cat, cathepsin; CF, cystic fibrosis; COPD, chronic obstructive pulmonary disease; CS, current smoker; CSE, cigarette smoke extract; ECM, extracellular matrix ; FEV, forced expiratory volume; FS, former smoker; GOLD, global initiative for chronic obstructive lung disease; hCAP, human cathelicidin antimicrobial peptide ; LHVS, morpholinourea-leucinyl-homophenylalanine-vinyl-sulfone; MMP, matrix metallo-proteinase; MMTS, S-methyl thiomethanesulfonate; NS, never-smoker; NSP, neutrophil serine proteases; pHBECs, primary human bronchial epithelial cells; PMSF, phenylmethylsulfonyl fluoride; ProCat, procathepsin.

Abstract:

Cigarette smoking has marked effects on lung tissue, including induction of oxidative stress, inflammatory cell recruitment and a protease/anti-protease imbalance. These effects contribute to tissue remodeling and destruction resulting in loss of lung function in chronic obstructive pulmonary disease (COPD) patients. Cathepsin S (CatS) is a cysteine protease that is involved in the remodeling/degradation of connective tissue and basement membrane. Aberrant expression or activity of CatS has been implicated in a variety of diseases, including arthritis, cancer, cardiovascular and lung diseases. However, little is known about the effect of cigarette smoking on both CatS expression and activity, as well as its role in smoking-related lung diseases. Here, we evaluated the expression and activity of human CatS in lung tissues from never-smokers and smokers with or without COPD. Despite the presence of an oxidizing environment, CatS expression and activity were significantly higher in current smokers (both non-COPD and COPD) compared to never-smokers, and correlated positively with smoking history. Moreover, we found that the exposure of primary human bronchial epithelial cells to cigarette smoke extract triggered the activation of P2X7 receptors, which in turns drives CatS upregulation. The present data suggest that excessive CatS expression and activity contribute, beside other proteases, to the deleterious effects of cigarette smoke on pulmonary homeostasis.

Keywords: cigarette smoke, COPD, cysteine protease, oxidation, smokers

Introduction:

Over 7 million deaths per year worldwide were recorded in 2017 that could be attributed to past or current smoking, and trends indicate that this will increase to 8 million annually by 2030 (63). Besides longtime smokers having a shorter life-expectancy (~10 years) compared with never-smokers (www.cdc.gov/tobacco/data_statistics), long-term effects of cigarette smoking include the risk of cardiovascular disease, lung cancer and chronic obstructive pulmonary disease (COPD), which is characterized by progressive and irreversible airflow obstruction. Conversely, cigarette smoking cessation improves substantially longevity in men and women, irrespective of the age (27, 59). Cigarette smoke exposure contributes to chronic airway inflammation and pathological lung tissue remodeling and destruction by increasing the recruitment of inflammatory cells such as neutrophils and macrophages (23, 45). The burden of oxidative stress associated with cigarette smoke exposure enhances recurrent bacterial infections and leads to a protease/anti-protease imbalance (12, 36).

The principal classes of proteases expressed in human lungs are serine proteases, matrix metalloproteases (MMP), and cysteine proteases (33). Lysosomal cysteine cathepsins are produced by a wide variety of cell types such as fibroblasts, macrophages, and epithelial cells, and these can be active outside lysosomes (secretory vesicles, cytosol, mitochondria, nucleus, and extracellular medium). Among them, cathepsins B, K, L, and S play important roles in diverse physiological events and are capable of degrading extracellular matrix (ECM) and basement membrane (BM) constituents as well as antimicrobial peptides (AMPs) (17). Besides MMPs and serine proteases, dysregulation of cysteine cathepsins expression may disrupt these normal biological processes and contribute to a number of diseases such as cancer, osteoporosis, arthritis, neurodegenerative and airway diseases (for review: (31, 43, 53, 54)). In particular, cathepsin S (CatS), which is predominantly expressed in dendritic cells and macrophages (antigen-presenting cells, APCs), and epithelial cells, is thought to play a pivotal role in chronic inflammatory lung diseases including cystic fibrosis (CF) and COPD (6, 28, 32, 56–58). Various studies have implicated CatS in extensive degradation of elastin fibers and collagens as well as in the cleavage and the inactivation of key antimicrobials in CF airways (for review: (17, 33)). Contrary to other related cathepsin family members that are rapidly inactivated at neutral pH, CatS remains stable, a property that enables it to be active extracellularly, particularly during ECM remodeling. Overexpression of CatS is observed in mouse models of experimental emphysema induced by IL-13 or IFN γ, and CatS inhibition by synthetic inhibitors reduces significantly the severity of emphysema and inflammation (18, 40, 55, 61). These data are supported by the observation that exposure of macrophages to

bronchoalveolar lavage fluid (BALF) from patients with COPD markedly increased CatS secretion, which was inhibited by IFN-γ neutralizing antibodies (19). This finding is in line with the observation that IFN-γ stimulates CatS expression and activity in various cell types, including keratinocytes and monocytes (20, 49). Interestingly, cigarette smoke enhanced the production of IL-18 (an IFN-γ inducing factor), and induced the expression of immuno-reactive CatS in lung macrophages of cigarette smoke-exposed mice as well as in lung tissues of patients with COPD (28).

Despite increasing evidence for a role of CatS in COPD experimental animal models, very little is known in human. Especially, the relationship between smoking status (current and former smokers) and history (pack-years) and human CatS expression and activity in the lungs of (ex)-smokers with or without COPD remains unsolved. Furthermore, the active site cysteine residue (Cys25, papain numbering) of thiol-dependent cathepsins is highly sensitive to oxidative reagents. The fact that CatS remains active in animal models and in COPD patients, raises the question of its resistance to unfavorable conditions due to CS-induced oxidative stress.

Therefore, in this report we compared both the protein levels and the enzymatic activity of human CatS in lung tissue from never-smokers, and current or ex-smokers with normal lung function or with various stages of COPD severity, according to the Global Initiative for Chronic Obstructive Lung Disease (GOLD) criteria (Gold I-III). Significantly higher levels of active CatS were detected in lung tissue from current smokers compared to never-smokers or former smokers. On the other hand, varying levels of CatS were detected in lung tissue from COPD patients that correlated with disease severity. To gain a better molecular understanding of the relationship between smoke exposure and CatS expression and activity, we used primary human bronchial epithelial cells (pHBECs) that were exposed to non-toxic doses of cigarette smoke extract (CSE). CSE increased the expression of CatS in pHBECs in a dose dependent-manner. Conversely, pharmacological inhibition of the purinergic P2X7 receptor, an ATP-gated cation channel, reduced CatS expression, which is in accordance with the fact that P2X7 plays a regulatory role in CatS expression as previously reported for human lung macrophages and mouse bone marrow-derived macrophages (35). Finally, even at high levels of CSE exposure, CatS activity was preserved suggesting that elastinolytic CatS may contribute in conjunction with other proteases to parenchymal destruction that is the hallmark of emphysema.

Material and methods:

Enzyme, substrates and inhibitors:

Human cysteine cathepsin S was supplied by Calbiochem (VWR International S.A.S., France) and its active site titration was determined using L-3-carboxy-trans-2, 3-epoxy-propionylleucylamide-(4-guanido)-butane (E-64) (Sigma-Aldrich, Saint-Quentin Fallavier, France). Unless stated, cathepsin activity assays were performed in acetate sodium buffer 100 mM, pH 5.5, dithiothreitol (DTT) 5 mM, and Brij35 0.01%. Benzyloxycarbonyl-Phe-Arg-7-amino-4-methyl coumarin (Z-Phe-Arg-AMC) and Benzyloxycarbonyl-Leu-Arg-7-amino-4-methyl coumarin (Z-Leu-Arg-AMC) were purchased from R&D System (R&D System Europe, Abingdon, UK). Benzyloxycarbonyl-Val-Leu-Arg-7-amino-4-methyl coumarin (Z-Val-Leu-Arg-AMC) was from AnaSpec (Eurogentec, Seraing, Belgium). DQ-elastin was purchased from Molecular Probes (Life Technologies, Saint Aubin, France). Pepstatin A, EDTA, AEBSF (Pefabloc), and S-methyl thiomethanesulfonate (MMTS) were from Sigma-Aldrich (Saint Quentin Fallavier, France). Morpholinourea-leucinyl-homophenylalanine-vinyl-sulfone phenyl inhibitor (LHVS) was a kind gift from Dr. J. H. McKerrow (Skaggs School of Pharmacy and Pharmaceutical Sciences, University of California, San Diego, CA, USA). The P2X7 antagonist 3-[1-[[(3'-Nitro[1, 1'-biphenyl]-4-yl)oxy]methyl]-3-(4-pyridinyl)propyl]-2, 4-thiazolidinedione (a.k.a. AZ 11645373) came from Tocris Bioscience (Bristol, UK).

Ethic statement: This study was conducted in accordance with the ethical standards set out in the Helsinki Declaration and the local French bioethical committee of The University Hospital Center, Trousseau Hospital, Tours, France (approval No. DC-2008-308), and informed consent was obtained for each patient.

Human lung tissue: Peripheral tumor-free lung tissue was collected from seventy-two patients who underwent surgery for non-small cell lung cancer between 2006 and 2011 (Trousseau Hospital, Tours, France), as previously described elsewhere (24). Clinical characteristics of these patients are described in **Table 1**. Non-tumor tissue was harvested at least 3 cm away from the tumor. The absence of carcinoma was checked histologically. Tissue samples were selected, reviewed for validation by the Department of Pathologic Anatomy and Cytology (The University Hospital Center, Tours, France). A diagnosis of COPD was made by the physician, based on smoking history (>20 pack-years) and forced expiratory volume in 1 s versus forced vital capacity (FEV_1/FVC) ratio of <0.7 using spirometry tests. According to the

global initiative for chronic obstructive lung disease (GOLD) staging, we reported 17 patients as having GOLD stage I, 18 as GOLD stage II, and 7 as GOLD stage III. Smoking history was calculated in pack-years, defined as the number of packs of cigarettes smoked per day multiplied by the number of years the person has smoked. Subjects were considered former smokers after cessation of smoking for at least one year before surgery. Upon collection, samples were quickly frozen in liquid nitrogen and stored at -80 °C. Tissue samples were embedded in Tissue-Tek OCT (Sakura Finetek Europe, Alphen aan de Rijn, The Netherlands) and 4 µm section were prepared using a cryotome (Thermo Scientific Inc., Waltham, MA, USA). Tissue sections were incubated in PBS or in a lysis buffer (20 mM Tris-HCl pH 8.0, 10% glycerol, 1% NP40, 2 mM EDTA, 137 mM NaCl) containing 200 mM sodium orthovanadate, a phosphatase inhibitor, and a cocktail of proteases inhibitors (10.4 mM AEBSF, 0.8 µM aprotinin, 40 µM bestatin, 140 µM E-64, 20 µM leupeptin, 15 µM pepstatin A). Incubation was made for 45 min at 4°C under agitation and then samples were centrifuged (21000xg) at 4°C for 20 min. Supernatants were harvested and frozen at -80°C until required. Protein quantification in supernatants was assessed with bicinchoninic acid assays (BCA protein assay kit, Interchim, Montluçon, France). Morphological analyses were performed using formalin-fixed paraffin-embedded lung tissues. The lung parenchyma and elastin fibers were stained with Hematoxilin-Eosin-Safran (HES) and with Orcein (Tissue-Tek Prisma, Sakura Finetek Europe), respectively. Prior to immunohistochemical staining, the paraffin wax was removed by xylene. Tissue sections were rehydrated by sequential washings with ethanol and with water, and next immersed in the Dako Target Retrieval solution (Dako France SAS, Les Ulis, France). Slides were heated (1 h at 56°C) then cooled according to the manufacturer's instructions, and first washed with water and next with PBS containing 0.2% (v/v) Tween 20. Endogenous peroxidase activities were neutralized by addition of hydrogen peroxide 3% for 10 min.

Immunohistochemical analysis of Cathepsin S in lung tissue

After washing (PBS containing 0.2% Tween 20), tissue sections were incubated with the polyclonal goat anti-human CatS antibody (1:100, Abcam, France) diluted in the Real Dako Antibody Diluent for 1 h at room temperature. The secondary biotinylated anti-goat antibody (Dako) was used to reveal binding of anti-CatS. Specificity of the staining was controlled by omission of the primary antibody. Staining was performed by the high-sensitivity substrate-chromogen system, Dako Liquid DAB (3, 3-diaminobenzidine tetrahydrachloride). In parallel, anti-cytokeratin 7 (a cytoplasmic marker that is confined to glandular and transitional

epithelial cells, 1:200, Dako), anti-thyroid transcription factor 1 (a nuclear marker, which located primarily in the nucleus of type II pneumocytes and club cells, 1:50, Dako) and anti-CD68 (a monocyte and macrophage marker, 1:200, Dako) were used as control. Hematoxylin was applied, and next the sample was dehydrated with alcohol. Finally, digital microscopic images were acquired (Nikon E600 optical microscope, magnification: x 400; Olympus DP70 camera) and processed with the Olympus DP Controller software. IHC staining controls were performed under the same conditions.

Western blotting and immunoassays: Goat polyclonal anti-human cathepsin S came from R&D System. The lack of cross reactivity with cathepsins B, K, L and H was checked as described elsewhere (46). Mouse monoclonal anti-β-actin was from Sigma-Aldrich. Anti-phospho-p38 MAPK (Thr180/Tyr182) rabbit monoclonal antibody was from Cell Signaling (Ozyme, Saint Quentin Yvelines, France) and anti-phospho-cPLA$_2$ (a.k.a. anti-phospho Ser505-cPLA$_2$) polyclonal rabbit antibody from Abcam (Paris, France). In order to prevent any bias associated with individual clinical specimen, tissue samples of each of the groups were equally pooled to deposit same amount of protein (30 μg) on 15% SDS-PAGE gels prior to be transferred onto nitrocellulose membranes (Hybond-ECL, Amersham Biosciences, Buckinghamshire, UK). The following groups were used: never-smokers, non-COPD current smokers, non-COPD former smokers, COPD current smokers at stages I, II and III, and COPD former smokers at stages I, II and III. Membranes were treated with antibodies (1:1000 in PBS, 0.1% Tween 20, 5% powdered milk) using standard Western-blot techniques, then incubated with corresponding (anti-goat, anti-mouse or anti-rabbit) secondary IgG-horseradish peroxidase conjugate (1:5000) for 1 h at room temperature prior to the detection using the ECL Plus Western Blotting (Amersham Biosciences). β-actin was used as an internal control of each protein sample, using β-actin antibody (1:2000) to ensure equal protein loading. Densitometric analysis of membranes was carried out using the ImageJ software (NIH, Bethesda, MD, USA). Data from tissue samples were normalized to β-actin signal. Assays were repeated at least three independent times. In addition, CatS concentrations were determined using sandwich ELISA DuoSet kit (R&D Systems) (measurement in triplicate).

Measurement of total anti-oxidant (TAS) and oxidant (TOS) status in lung tissues: TAS and TOS levels in tissue sample (5 μg) were measured by Erel's methods (15, 16) according to the instructions of the manufacturer (Rel Assay Diagnostics; Mega Tip, Gaziantep, Turkey).

Briefly, TAS method depends on the ability of antioxidants present in the sample to inhibit $ABTS^{+}$ radical cation formation from the oxidation of ABTS (2, 2′-azino-di-3-ethylbenzthiazoline-6-sulfonic acid) by metmyoglobin and hydrogen peroxide. The assay is calibrated with a standard stable antioxidant solution of known concentration, referred to as Trolox equivalent (6-hydroxy-2, 5, 7, 8-tetramethylchroman-2-carboxylic acid; a soluble vitamin E analog). Values of TAS are expressed as μmol Trolox equivalent/liter (μmol Trolox eq./L). The TOS method is used to assess the total amount of oxidant molecules present in the sample and is based on the capacity of oxidants in the sample to oxidize the ferrous ion-chelator complex to ferric ions, generating a colored complex with xylenol orange in an acidic medium (Abs = 530 nm). The TOS assay is calibrated with hydrogen peroxide (H_2O_2) and the results were expressed in μmol H_2O_2 eq./L.

Active site titration of cathepsin S and elastinolytic activity in lung tissues: Active site titration of CatS as well as measurement of the total endopeptidase cysteine cathepsin activity in lung tissue samples was adapted from a previous report (42). As CatS is more stable than the other cathepsins at neutral pH, its specific activity was assayed under neutral condition. Tissue samples (5 μg of total protein) were incubated in 100 mM sodium-phosphate buffer pH 7.4 for 1 h at 37°C to inactivate the other endopeptidase cathepsins. An aliquot was then removed, diluted with 100 mM sodium-acetate buffer pH 5.5, 10 mM DTT and Brij35 0.01% and used to measure the CatS activity at 37°C with Z-Val-Leu-Arg-AMC (20 μM) in the presence of increasing concentration of E-64 (0-500 nM). The CatS activity was monitored using excitation and emission wavelengths of 350 nm and 460 nm (Gemini spectrofluorimeter, Molecular Devices) in 96-well Nunc microtiter plates (ThermoFisher Scientific, Illkirch, France) under gentle agitation. Measurement of CatS elastinolytic activity was made using DQ-elastin (25 μg) as substrate (excitation and emission wavelengths of 480 nm and 530 nm, respectively). Controls were performed with the inhibitor LHVS (100 nM).

Preparation of aqueous cigarette smoke extract (CSE): CSE was prepared using a protocol modified from (47). Mainstream smoke of three Research-grade cigarettes (3R4F) with filter (Kentucky Tobacco Research and Development Center at the University of Kentucky, Lexington, KY) was bubbled in 100 mM sodium acetate buffer, pH 5.5 (50 mL) or in 100 mM HEPES buffer, pH 7.4 (50 mL) in a closed environment. The average burning time per cigarettes was about 8 min. The obtained solution was considered as 100% CSE and was

aliquoted and stored at -80°C until required. CSE preparation was standardized by measuring the absorbance at 320 nm (corresponding to the absorbance of polycyclic compounds, e.g. quinic acid or nicotine) with a Cary 100 UV visible spectrophotometer (Agilent Technologies, Courtaboeuf, France). CSE (100%) designed for cell culture was generated in BEBM media (Lonza, Workingham, UK) and sterile-filtered through a 0.2 µm filter, as previously described ((47)).

Oxidative potential of CSE: The oxidative potential of CSE was determined by the redox conversion of reduced (non-fluorescent) dihydro-rhodamine-123 to oxidized (fluorescent) rhodamine-123 (Sigma-Aldrich) (21). Briefly, CSE (0 to 40%) was incubated in 100 mM sodium acetate buffer, pH 5.5 with dihydro-rhodamine-123 (50 µM) protected from light for 1 h at room temperature. Since CatS is stable and active at neutral pH, similar assays were performed in 100 mM HEPES buffer, pH 7.4. Released fluorescence was then measured using a Cary Eclipse spectrofluorimeter (Agilent Technologies, Les Ulis, France; excitation wavelength: 490 nm, emission wavelength: 530 nm), and quantified using a calibration curve of rhodamine-123 (0 to 200 nM).

Treatment of primary human bronchial epithelial cells (pHBECs) by CSE and cytoxicity assays: Normal primary human bronchial epithelial cells (pHBECs, Lonza) from three different donors were seeded at passage 3 in 60 mm dishes at a density of 10000 cells/cm² in BEGM medium (Lonza) with supplements and antibiotics, and allowed to reach confluence (~7 days). Then cells were treated with CSE (0-50%) for 2 h and 24 h in a total amount of 5 mL media. The viability of CSE treated cells was assessed by lactacte deshydrogenase (LDH) assay as reported elsewhere (47). Briefly, the activity of released LDH in cell culture supernatant was assessed with the cytotoxicity detection kit (LDH) (Roche, Mannheim, Germany) following the manufacturer's instructions and cell viability calculated accordingly. Also, a control experiment was carried out by measuring the increase of cytochrome P450 1 A1 (CYP1A1), in the presence of CSE. Real-time quantitative PCR analysis of CYP1A1 mRNA was performed as previously reported (48, 51). Oxidative stress within the cells (10^4 cells/cm²) was measured using MitoSOX Red mitochondrial superoxide indicator (Molecular Probes, Invitrogen, Karlsruhe, Germany). Medium was aspirated from the cell layer and 5 µM MitoSOX master mix, prepared in BEGM medium, was added onto the cells followed by 30 min incubation at 37°C. The cell layer was washed three times with 0.5 mL of HBSS buffer (Lonza) (37°C) and the cells trypsinized with 0.3 mL trypsin (Lonza) followed by

addition of trypsin inhibitor TNS (Lonza) when cells were detached. Cells were pelleted, washed once with HBSS and resuspended in 0.4 mL fluorescence-activated cell sorting (FACS) buffer (PBS, 2% FBS, 20 μM EDTA). Data acquisition was performed in a BD LSR II flow cytometer (BD Bioscience, San Jose, CA, USA). Cells were gated for singlets and superoxide production measured as mean MitoSOX fluorescence. As positive control, antimycin A (70 μM) was added to the untreated sample after the FACS measurement and measured after 10 min. Quantification of mean fluorescence was performed in BD FACSDiva 8.0 software (BD Bioscience).

Preparation of pHBECs extracts: Culture media were then harvested and treated immediately with 100 mM sodium acetate, pH 5.0, 0.5 mM PMSF, 0.5 mM EDTA, 40 μM pepstatin A, 1 mM MMTS (preservative buffer). Cell debris were removed by centrifugation (1000xg, 8 min, 4°C). Supernatant was concentrated by centrifugal ultrafiltration (Vivaspin 4, Sartorius, Dourdan, France) and next stored at -80°C pending analysis. Alternatively, plated cells were washed twice with ice-cold PBS and scraped in the preservative buffer. Total cell extracts were obtained by a series of three freeze/thaw cycles. Cell lysates were centrifuged (5000xg at 4°C for 10 min), and cell lysate supernatants were collected and frozen at -80 °C. Protein quantification was assessed by Bradford assay (Biorad). Titration of the endopeptidase cysteine cathepsin activity was performed with E-64 as previously described (42). Cell-lysate supernatants (5 μg of total protein) were subjected to 15% SDS-PAGE under reducing conditions and immunoblotted as described above using anti-CatS, anti-phospho-p38 MAPK and anti-phospho-cPLA$_2$ antibodies (1:1000).

Hydrolysis of LL-37 by pHBECs: Synthetic LL-37 (20 ng, GeneCust Europe, Dudelange, Luxembourg) was incubated with cell-lysate supernatants from pHBECs, (0.2 μg of total protein) treated or not with 10% CSE, in 100 mM sodium acetate buffer pH 5.5 for 0-24 h at 37°C, in the presence or absence of E-64 (10 μM) or LHVS (100 nM). Cell-lysate supernatants were subjected to 15% SDS-PAGE under reducing conditions and immunoblotted as described above using a rabbit polyclonal anti-LL-37 antibody (1:10000, Innovagen, Lund, Sweden).

Treament of pHBECs with P2X7 antagonist: Confluent pHBECs were pre-incubated with AZ 11645373, a highly specific P2X7 antagonist (1 μM, Tocris Bioscience) or mock (DMSO) for 1 h, before exposure for 2 h to 2.5 % CSE. Culture media were then harvested and treated as

reported in the previous paragraph. Titration of cathepsins was performed with E-64. Cell-lysate supernatants were subjected to 15% SDS-PAGE under reducing conditions and immunoblotted using anti-CatS antibody (R&D system, 1:1000).

Modulation of the enzymatic activity of CatS by CSE: The activity of CatS (1 nM) was measured *in vitro* at 37 °C in the presence of increasing amounts of CSE (0-40%) in 100 mM sodium acetate buffer, pH 5.5, 0.01% Brij35, 15 µM DTT, using Z-Leu-Arg-AMC (20 µM) as substrate. Experiments were performed in 96-well microtitration plates (Nunc, microtiter plates, ThermoFisher Scientific, France) and fluorescence release was monitored using a Spectramax Gemini spectrofluorimeter (excitation wavelength: 350 nm, emission wavelength: 460 nm). Under these experimental conditions, the substrate consumption was less than 5%. The same assays were repeated in 100 mM HEPES buffer, pH 7.4, 0.01% Brij35, 15 µM DTT in the presence of CSE (0-40%). All kinetic measurements were performed in triplicates and repeated twice.

Statistical analysis: Data were expressed as mean ± SD unless indicated. Statistical significance between the different values was analyzed by non-parametric Mann-Whitney U test and groups comparison were performed with non-parametric Kruskal-Wallis test (Dunn's multiple comparisons). Statistical analysis was performed using GraphPad Prism 7 (GraphPad software, San Diego, CA, USA). Differences at a p-value < 0.05 were considered significant.

Results

Clinical data of patients undergoing lung resection

Seventy-two patients were enrolled for this study and divided into nine groups based on their smoking status. Their clinical characteristics are summarized in **Table 1**. There were no significant differences in mean age between groups, except between non-COPD current smokers (CS) and never-smokers (NS) group (p=0.004). The number of pack-years was similar (no statistically significant difference) in all groups of smokers (including CS and former smokers (FS) with or without COPD) with a median of 40 pack-years smoking. The GOLD system categorizes airflow limitation into stages: GOLD I is mild with a FEV_1 (forced expiratory volume in one second, % predicted) ≥ 80%, GOLD II is moderate (50% ≤FEV_1 <80% predicted) and Gold III is severe (30% ≤FEV_1 <50% predicted). Here, FEV_1 in GOLD stage II and III patients was significantly lower compared to non-COPD patients and GOLD stage I patients ($p<0.05$).

Detection of cathepsin S by IHC in lung tissue of smokers

To ascertain CatS expression, immunohistochemistry (IHC) was performed on formalin-fixed, paraffin-embedded lung tissue sections from selected patients of the cohort (NS, non-COPD CS, and CS with COPD) (**Fig. 1A**). Modest levels of immunoreactive CatS was observed in the lungs of NS, while higher expression of CatS was readily detected in non-COPD CS and CS with COPD. Highest expression of CatS was observed in the bronchial epithelial layer, type II pneumocytes and alveolar macrophages. CatS immunoreactivity was also detected in submucosal glands, while non-ciliated club cells of the bronchiolar epithelium were weakly stained. The degradation of the lung interstitium by elastinolytic proteases including CatS is a critical factor in the pathogenesis of cigarette smoke-induced emphysema. Accordingly, more areas with interruption and fragmentation of elastin fibers in lung tissue from non-COPD CS and CS with COPD compared with NS were observed.

Cathepsin S levels in lung tissue of never-smokers and smokers

Then, we expanded previous observations by comparing CatS levels in a cohort of 72 patients, including NS (n=10), smokers (n=62, including CS and FS with and without COPD). Western-blot analysis confirmed a higher CatS protein expression in selected samples of non-COPD and COPD smokers *versus* NS (**Fig. 1B**). While the mature form of CatS (25 kDa) was strongly stained, staining of its proform was fainter. Moreover, levels of immunoreactive CatS

402 determined by ELISA was significantly ~2.5-fold higher in lung tissue lysates from the
403 cohort of cigarette smokers compared to NS (p=0.0033) (**Fig. 1C**).
404
405 *Active smoking is associated with increased pulmonary cathepsin S expression*
406 To evaluate whether CatS expression might be correlated with the smoking status and history,
407 we compared specifically the levels of CatS by ELISA in lung tissue samples from each NS,
408 CS and FS with or without COPD (**Fig. 2**). Levels of CatS were significantly higher (~4-fold)
409 in lung tissue from non-COPD CS and COPD CS than those from NS, while FS expressed
410 lower levels (~1.5-fold) of CatS (**Fig. 2A**). Interestingly, a ~2-fold decrease of CatS
411 expression was measured in non-COPD FS and COPD FS compared with CS ($p<0.05$ for
412 each comparison). Pack-years of cigarette smoking correlated positively with lung CatS
413 expression ($r_s = 0.468$, $p = 0.012$, **Fig. 2B**) in the cohort that encompasses NS and CS with and
414 without COPD, while CatS expression correlated negatively with FEV_1 (% predicted) ($r_s = -$
415 0.5337, $p = 0.0041$, **Fig. 2C).** However, no significant relationship between CatS expression
416 and the number of pack-years or FEV_1 was found with non-COPD FS and FS with COPD.
417 Nevertheless, the number of pack-years correlated negatively with FEV_1 (%) in the cohort of
418 72 patients ($r_s = -0.429$, $p = 0.0002$) (**Fig. 2D**). This suggests that overexpression of CatS in
419 CS is mostly associated with the number of pack-years smoking and is inversely related to a
420 decline in lung function.
421
422 *Cathepsin S expression and COPD severity*
423 To extend our analysis of the relationship between COPD severity and CatS expression, we
424 further subdivided FS and CS with COPD into three groups based on their GOLD stages (I:
425 mild, II: moderate and III: severe) and investigated expression of CatS by Western-blot and
426 densitometry analysis (**Fig. 2E)**. Mature CatS from pooled samples from CS with COPD was
427 significantly higher (~3-fold for GOLD I, II and ~5-fold for GOLD III), compared to NS
428 ($p<0.05$), while its expression was lower in FS with COPD. This result was further confirmed
429 by ELISA, which was performed for each lung tissue sample (**Fig. 2F, 2G)**. There was a
430 tendency toward an increase of CatS levels depending on the severity of COPD in CS, but not
431 in FS with COPD. Interestingly the negative correlation between CatS expression and FEV_1
432 was significantly higher in CS with GOLD I, II and III subgroups ($r_s = -0.5428$, $p = 0.0061$),
433 and even more when analysis was focused on CS with moderate and severe stages of COPD

(i.e. GOLD II and III) ($r_s = -0.6043$, $p = 0.0079$). No significant correlation was found between FEV_1 and the cohort that encompasses NS and CS without COPD.

Oxidative state in lung tissues of smokers

Based on the induction of oxidative stress by cigarette smoke (11) and our observation that CatS expression was higher in current smokers, we next investigated total oxidant status (TOS) and total antioxidant status (TAS) in lung tissue samples (**Table 2**). The values of TOS and oxidative stress index (OSI = TOS/TAS) in both non-COPD CS and CS with COPD groups were significantly higher than that in NS group ($p<0.05$; $p<0.0001$, respectively). In contrast, values of TAS were significantly lower in both non-COPD CS and CS with COPD compared to NS ($p<0.05$).

Active smoking is associated with increased cathepsin S activity in lung tissue of smokers

Consistent with immunoassays (ELISA and Western-blot data), CatS peptidase activity was significantly higher in non-COPD CS ($p=0.0016$) and CS with COPD ($p=0.0025$) compared to NS, while FS expressed significant lower levels of active CatS (**Fig. 3A**). Measurement of CatS activity supported that there was also a trend for an increase of CatS levels that is specifically associated to the severity of COPD only in CS patients (**Fig. 3B, 3C**). Especially, a significant ~4-fold higher of CatS activity was found in GOLD III CS compared to NS ($p<0.05$). Concomitantly, a significant increase of the elastinolytic activity of CatS was observed in smokers (including CS, FS without and with COPD) compared to NS ($p=0.0002$), using a fluorescein-labeled elastin (DQ-elastin) (**Fig. 3D**). Hydrolysis of DQ-elastin was impaired by morpholinourea-leucinyl-homophenylalanine-vinyl-sulfone (LHVS), a selective inhibitor of CatS, supporting that overexpressed CatS may contribute to matrix remodeling in smokers. Finally, levels of CatS peptidase activity in both non-COPD CS and CS with COPD correlated positively with the number of pack-years ($r_s = 0.419$, $p = 0.0063$) (**Fig. 3E**) and negatively with FEV_1 (% predicted) ($r_s = -0.381$, $p = 0.046$**, Fig 3F**). No significant correlation was observed between CatS activity and FEV_1 in the subgroups of CS or FS without COPD, contrary to CS with COPD (Gold I, II, III) cohorts ($r_s = -0.3981$, $p = 0.048$).

Cigarette smoke-induced cathepsin S expression and activity in primary human bronchial epithelial cells

CatS has a restricted tissue distribution with a major expression in antigen presenting cells (i.e. dendritic cells, macrophages) but also in airway epithelial cells (52, 56). Accordingly, we investigated whether CSE could induce overproduction of active CatS in primary human bronchial epithelial cells (pHBECs) (**Figure 4**). To pinpoint non-toxic doses of CSE, we treated pHBECs with a range of CSE concentrations (0%, 5%, 10%, 25%, and 50%) for up to 24 h and assessed cell viability by LDH assay (Fig. 4A) and cell morphology (Fig. 4B). No signs of toxicity were observed even in high dose of CSE-exposed pHBECs compared to untreated cells after 2 h, since only 50% CSE treatment exerted a significant lethal effect on cells after 24 h treatment (Fig. 4A). Inverted microscopy confirmed that pHBEC cell morphology was not changed after 2 h and 24 h of CSE stimulation, except for 50% CSE-exposed cells for 24 h, which were rounded up and were detached from the culture plates (Fig. 4B). Therefore, a concentration range of CSE (2.5-20%) was used in all subsequent experiments for a time period of 2 h incubation. In addition, a control experiment was carried out beforehand to check the effectiveness of the exposure of pHBECs to CSE by measuring the increase of cytochrome P450 1 A1 (CYP1A1), which is associated with oxidative stress response (26). This preliminary analysis confirmed that CYP1A1 mRNA expression was ~4-fold upregulated in pHBECs after 2 h treatment with CSE (2.5%, 5%, 10%, and 20%) compared to untreated cells. Next, to ascertain that CSE induced oxidative stress in pHBECs, we evaluated mitochondrial reactive oxygen species (mtROS) levels using MitoSOX-based flow cytometry. As shown in Figure 4C, CSE induced mtROS production in pHBECs, which was significant (~2-fold increase, $p=0.0094$) in 20% CSE exposed-cells compared to untreated cells, supporting that the different CSE preparations used were active on pHBECs even during a short period of exposure. After 2 h of CSE exposure, we observed by immunochemical techniques (Western-blot and ELISA) a dose-dependent increase of intracellular CatS (**Fig. 5A, B**). E-64 titration demonstrated that the concentration of active cysteine cathepsins was significantly higher in 20% CSE-exposed cells (32.8 ± 4.2 nmol/mg of total protein) compared to untreated cells (22.0 ± 3.6 nmol/mg of total protein) ($p<0.01$), although we failed to determine the specific concentration of active CatS. Accordingly, we measured a dose-dependent spread of the overall peptidase activity of cathepsins toward Z-Phe-Arg-AMC in pHBECs lysates ($r^2=0.81$, $p<0.05$) (**Fig. 5C**). In a previous report, we demonstrated that CatS cleaved and inactivated in a specific manner the antimicrobial peptide LL-37 (1). We therefore incubated exogenous LL-37 with 10% CSE-exposed pHBECs lysates for 6 and 24 h to provide further evidence of CatS activity in pHBECs. A time-dependent loss of immunoreactive LL-37 was observed (**Fig. 5D**). Conversely addition of LHVS (100 nM)

prevented hydrolysis of LL-37 by pHBECs lysates, supporting that LL-37 degradation relied on the overexpression of CatS triggered by exposure to 10% CSE.

Cigarette smoke-induced increase in cathepsin S is mediated by the P2X7 receptor in primary human bronchial epithelial cells

According to previous reports (5, 13), we hypothesized that CSE could drive the calcium-dependent $cPLA_2$-induced lysosomal secretion of CatS, via the activation of the P2X7 receptor. Thus, pHBECs were treated with 2.5% CSE for 2 h in the presence or absence of a P2X7 receptor antagonist (AZ 11645373). Subsequent Western-blot densitometric analysis indicated that P2X7 antagonist significantly reduced ($p<0.05$) by approximately 7-fold the level of CatS (**Fig. 5E**). Likewise, a quantitative analysis by ELISA reinforced that the level of immunoreactive CatS was below the experimental limit of detection (<15.6 pg/mL) in P2X7 antagonist-treated pHBECs (data not shown) compared to that measured in 2.5% CSE-exposed pHBECs (37.85±15 pg/mL). Additionally, previous reports demonstrated that the exposure to cigarette smoke induces a compelling increase of phosphorylation of p38 MAPK and $cPLA_2$ (10, 62). Consistent with these findings, we observed that CSE triggered the phosphorylation of both p38 MPAK and $cPLA_2$ expression in dose-dependent manner in pHBECs (**Fig. 5F**). Taken together with previous reports, our data support that the CSE-induced upregulation of CatS is partly mediated by the MAPK signaling pathway, through P2X7 receptor activation in pHBECs (**Fig. 6**).

Partial inactivation of cathepsin S by cigarette smoke extract

Due to its low pKa, the active-site thiol of cysteine cathepsins is highly sensitive to redox modifications, resulting in a decreased proteolytic activity (21). Nevertheless, active CatS is still found in lung tissue of smokers and CSE-exposed pHBECs despite an unfavorable oxidizing environment. Given these apparently contrasting observations, we studied the effect of increasing amounts of CSE on activity of CatS at pH 5.5 and 7.4 *in vitro*. First, CSE solutions (2.5-40%) were quantified and calibrated by measurement of their absorbance (320 nm) and by assessment of their capacity to oxidize dihydrorhodamine-123 (non-fluorescent) into rhodamine-123 (λ_{exc}: 490 nm, λ_{em}: 530 nm) (39), as described in the experimental section (**Fig. 7A and 7B**). CSE partially inactivated CatS in a time- and concentration-dependent manner (**Fig. 7C**). Nevertheless, CatS was less sensitive to inactivation by CSE at pH 7.4 than pH 5.5 (**Fig. 7D**), likely due to a ~2-fold decrease of CSE oxidative potential at pH 7.4 (**Fig. 7B**). Although neutral pH and oxidative stress are believed to be a major drawback for the

extracellular activity of cysteine cathepsins, present results confirm that CatS exposed to oxidizing CS may partly retain its enzymatic activity.

Discussion

In the present study, we examined the expression and activity of CatS in lung tissue of 72 patients including never-smokers, smokers with or without COPD, and related this to their smoking status and history, and lung function. Increased levels of active CatS were measured in cancer-free parenchymal lung tissue samples from smokers compared to never-smokers. CatS increase was prominent comparing CS *vs* NS, nevertheless FS displayed markedly lower levels of CatS than CS, which is in line with the hypothesis that active smoking may drive CatS expression in lung tissue.

To our knowledge, this is the first report that establishes a comprehensive relationship between both CatS expression and activity in human lungs, and cigarette smoking. We highlighted a specific increase of CatS in lung tissue samples from current smokers, suggesting that CatS levels correlate to smoking history and may contribute to smoking-induced lung injury. Also results are consistent with a former study, using a semi-quantitative IHC approach, which reported that CatS protein levels in lung tissues differ between current and former smokers (28). Although the present cohort of patients was not suited to determine the minimal exposure time to cigarette smoke leading to the enhancement of CatS expression in the lungs of smokers, we found that CatS overexpression correlates positively with cumulative cigarette exposure (pack-years) in current smokers, but not former smokers. Conversely no significant differences in CatS levels were observed between non-COPD and COPD smokers. This most likely reflects that besides upregulation of CatS activity during COPD, additional proinflammatory mediators (e.g. cytokines, chemokines, growth factors, oxidants and lipid mediators) secreted by inflammatory cells (i.e. alveolar macrophages, neutrophils, and T lymphocytes) and also by epithelial and endothelial cells and fibroblasts from lung airway are involved in orchestrating the progressive airflow limitation and alveolar destruction (emphysema) in patients with COPD (for review: (3)). Nevertheless, variations in CatS protein and activity levels that related to GOLD stages were observed only in current smokers. Moreover, both CatS protein and activity levels were markedly elevated in severe (stage III) COPD patients compared to NS. Present results must be interpreted with caution and will deserve further investigations with a larger cohort of COPD patients with different Gold stages (I-IV). Though, this finding is in line with a previous study showing that mature CatS levels are higher in bronchoalveolar lavage fluid from COPD patients compared with

healthy volunteers (19). Likewise, plasma CatS level was also higher in severe COPD patients compared with healthy smokers (CS) and never-smokers (41). Nevertheless, plasma CatS level did not correlate with the severity of the disease among the COPD patients, probably due to the presence of former smokers among COPD patients enrolled in the study. Finally, a crucial remaining issue is to establish whether active CatS up-regulation may be associated with emphysema severity during COPD.

One concern is that all the resected samples for the study came from patients who all underwent surgery for primary lung cancer. Under these circumstances, the present analysis was restricted to tumor-free lung tissues in order to restrain potential biases due to tumoral environment. On the other hand, we observed a statistically significant correlation between the severity of airflow obstruction (FEV_1) and CatS expression/activity in lung tissues from current smokers with COPD. Accordingly, an elegant study has demonstrated that the increase of both CatS activity and protein levels in BALF from patients with cystic fibrosis (CF) is associated with lower lung function (56). Hence, one could speculate that, besides development and progression of COPD in smokers, upregulation of CatS may also be linked to other chronic airway inflammatory disorders. About 40% of "heavy" smokers (>1 pack of cigarettes per day) develop emphysema (25), and increased CatS may contribute to extensive breakdown of parenchymal lung tissue. Although cessation of smoking produces a considerable decrease in COPD mortality, there is growing evidence that the rate of decline of lung function continues, suggesting that irreversible changes occur with long-lasting effects. Despite lower active CatS levels were found in former smoker (non-COPD and COPD) compared to current smokers (non-COPD and COPD), they were still higher than in never-smokers, which may contribute to persistent inflammation and to some extent to lung parenchyma destruction with reduced lung function for some individuals. A number of studies have investigated elastin degradation *in vitro* by lysosomal cysteine cathepsins, and showed that the elastinolytic activities of CatS and CatK, and to a less extent of CatL, are comparable or higher than those of neutrophil elastase and MMPs, strengthening their pivotal role in matrix degradation and remodeling (7–9, 22, 38). Also, among cysteine proteases expressed in lungs, CatS has the unique property to efficiently degrade elastin fibers at both pH 5.5 and 7.4 (50), and *in vivo* studies demonstrated the capacity of CatS to cause airspace enlargement in mice (55, 60). Here we demonstrated that the specific CatS-mediated elastinolytic activity was critically increased in lung extracts of smokers compared to never-smokers. Similar findings showing an increased activity of CatS associated to smoke-exposure were found using rodent experimental models of smoke-exposed guinea pigs and mice (22, 28). Cigarette

smoke-exposed animals developed emphysema with a significantly extensive decrease of ECM content (collagen and elastin) (22). Of note, no CT scanning and/or diffusion lung capacity for carbon monoxide (DLCO) were performed in this study to evaluate emphysema in the cohort of patients.

Concordantly, a fragment of decorin, one of the most abundant proteoglycans of the ECM, was identified in the serum of patients with COPD or fibrotic lung disorders (29). This decorin-derived peptide that is specifically released by CatS was proposed as a valuable serum biomarker for these lung disorders (29).

Despite the fact that CatS has a restricted cellular distribution with a prevalent expression in APCs, there is evidence that other lung cells also produce CatS (30, 52, 56). Present IHC studies revealed that the increased immunoreactivity of CatS in peripheral lung tissue of current smokers is also assigned to type II pneumocytes and bronchial epithelial cells. We demonstrated that exposure of primary human bronchial epithelial cells (pHBECs) to CSE rapidly induced a dose-dependent increase of CatS expression. It was shown that CSE exposure triggers the release of ATP from pHBECs via the sequential activation of transient receptor potential cation channels of the vanilloid subtype (TRPV) 1 and 4 and pannexin-1 channel pore, respectively (5). Likewise, ATP acts on the purinergic receptor P2X7, that plays a pivotal role in cigarette smoke-induced lung inflammation and emphysema (5, 37). Interestingly, lipopolysaccharide combined with high concentration of ATP (millimolar concentrations) promotes rapidly (<4 h) the release of active CatS from microglial lysosomes, via P2X7 receptor activation as well as the downstream activation of p38 MAPK and cytosolic phospholipase A2 ($cPLA_2$) (13). Furthermore, it has been reported that the levels of extracellular ATP, proinflammatory cytokines including IL-18, and P2X7 receptor are increased in the airways of both non-COPD and COPD smokers and may contribute to the pathogenesis of smoking-related lung diseases (14, 34, 44). Interestingly, extracellular ATP rapidly enhanced the expression of active CatS from microglia, a process that involved P2X7 receptor activation and downstream activation of p38 MAPK and $cPLA_2$, which plays a crucial role in membrane fusion during lysosome exocytosis (2, 13). Consequently, data presented herein suggest a crucial role for P2X7 receptor, also implying p38 MAPK and $cPLA_2$ signaling pathways, in the release of CatS in pHBECs in response to CSE exposure (Fig. 6). The present study supports that cigarette smoke-activation of P2X7 receptor may contribute to lung tissue damage through the release of CatS.

A number of studies have investigated the potential benefits of P2X7 blockade in rodent models of inflammatory disorders, including neurologic inflammation, rheumatoid arthritis,

bone cancer and COPD (for review: (4)). It can be speculated that treatment with specific P2X7 antagonists may reduce the release of CatS and could account for the reduction of lung symptoms in heavy smokers with or without COPD. Alternatively, the potentially harmful actions of CatS in autoimmune and inflammatory chronic diseases is well established, suggesting its inhibition by selective and specific drugs may be crucial for patient outcome. Several studies have validated the safety and clinical efficacy of such inhibitors in preclinical models and clinical studies for the treatment of rheumatoid arthritis, skin diseases and neuropathic pain (for review: (57)). The emerging role of CatS deregulation in smoking-related lung diseases may pave the way for the development of further CatS inhibitors, which hopefully may represent a modulatory strategy for treating in part emphysema by limiting elastic fiber destruction.

Acknowledgments

We are grateful to Dr Aurelia Barascu and Dr Fabien Gueugnon, who both managed the collection of lung tissue samples. Mu-Leu-Hph-VSPh (CatS inhibitor) was kindly provided by Professor James H. McKerrow (Skaggs School of Pharmacy and Pharmaceutical Sciences, University of California, San Diego, CA, USA). We also acknowledge Professor Pieter Hiemstra (Leiden University Medical Center, Leiden, The Netherlands) for a critical review of the manuscript. P. Hiemstra is currently a visiting scientist at INSERM UMR 1100 (Le Studium grant, Région Centre-Val de Loire, France). Dr P-M. Andrault was a recipient of a doctoral grant from Institut National de la Santé et de la Recherche Médicale (INSERM)-Région Centre-Val de Loire, France. T. Chazeirat is a recipient of a doctoral grant from University of Tours. Dr. M. Wartenberg was a doctoral recipient from Région Centre-Val de Loire. This work was supported by institutional funding from INSERM, by a grant from Région Centre-Val de Loire (project BPCO-LYSE #2015103986), and by the Deutsche Forschungsgemeinschaft (DFG) within the Research Training Group DFG GRK2338 (grant to CASW), the Helmholtz Association, and the Comprehensive Pneumology Center Research School “Lung Biology and Disease”. These agencies played no role in study design, data collection and analysis, the decision to publish or preparation of the manuscript.

References

1. **Andrault P-M**, **Samsonov SA**, **Weber G**, **Coquet L**, **Nazmi K**, **Bolscher JGM**, **Lalmanach A-C**, **Jouenne T**, **Brömme D**, **Pisabarro MT**, **Lalmanach G**, **Lecaille F**. Antimicrobial Peptide LL-37 Is Both a Substrate of Cathepsins S and K and a Selective Inhibitor of Cathepsin L. *Biochemistry* 54: 2785–2798, 2015.

2. **Andrei C**, **Margiocco P**, **Poggi A**, **Lotti LV**, **Torrisi MR**, **Rubartelli A**. Phospholipases C and A2 control lysosome-mediated IL-1 beta secretion: Implications for inflammatory processes. *Proc Natl Acad Sci U S A* 101: 9745–9750, 2004.

3. **Barnes PJ**. Cellular and molecular mechanisms of asthma and COPD. *Clin Sci* 131: 1541–1558, 2017.

4. **Bartlett R**, **Stokes L**, **Sluyter R**. The P2X7 receptor channel: recent developments and the use of P2X7 antagonists in models of disease. *Pharmacol Rev* 66: 638–675, 2014.

5. **Baxter M**, **Eltom S**, **Dekkak B**, **Yew-Booth L**, **Dubuis ED**, **Maher SA**, **Belvisi MG**, **Birrell MA**. Role of transient receptor potential and pannexin channels in cigarette smoke-triggered ATP release in the lung. *Thorax* 69: 1080–1089, 2014.

6. **Brömme D**, **Wilson S**. Role of Cysteine Cathepsins in Extracellular Proteolysis [Online]. In: *Extracellular Matrix Degradation*, edited by Parks WC, Mecham RP. Springer Berlin Heidelberg, p. 23–51. http://link.springer.com/10.1007/978-3-642-16861-1_2 [28 Jun. 2015].

7. **Bühling F**, **Röcken C**, **Brasch F**, **Hartig R**, **Yasuda Y**, **Saftig P**, **Brömme D**, **Welte T**. Pivotal Role of Cathepsin K in Lung Fibrosis. *Am J Pathol* 164: 2203–2216, 2004.

8. **Chapman HA**, **Munger JS**, **Shi GP**. The role of thiol proteases in tissue injury and remodeling. *Am J Respir Crit Care Med* 150: S155-159, 1994.

9. **Chapman HA**, **Riese RJ**, **Shi GP**. Emerging roles for cysteine proteases in human biology. *Annu Rev Physiol* 59: 63–88, 1997.

10. **Cheng S-E**, **Lin C-C**, **Lee I-T**, **Hsu C-K**, **Kou YR**, **Yang C-M**. Cigarette smoke extract regulates cytosolic phospholipase A2 expression via NADPH oxidase/MAPKs/AP-1 and p300 in human tracheal smooth muscle cells. *J Cell Biochem* 112: 589–599, 2011.

11. **Church DF**, **Pryor WA**. Free-radical chemistry of cigarette smoke and its toxicological implications. *Environ Health Perspect* 64: 111–126, 1985.

12. **Churg A**, **Cosio M**, **Wright JL**. Mechanisms of cigarette smoke-induced COPD: insights from animal models. *Am J Physiol Lung Cell Mol Physiol* 294: L612-631, 2008.

13. **Clark AK**, **Wodarski R**, **Guida F**, **Sasso O**, **Malcangio M**. Cathepsin S release from primary cultured microglia is regulated by the P2X7 receptor. *Glia* 58: 1710–1726, 2010.

14. **Eltom S**, **Stevenson CS**, **Rastrick J**, **Dale N**, **Raemdonck K**, **Wong S**, **Catley MC**, **Belvisi MG**, **Birrell MA**. P2X7 receptor and caspase 1 activation are central to airway inflammation observed after exposure to tobacco smoke. *PloS One* 6: e24097, 2011.

15. **Erel O**. A novel automated method to measure total antioxidant response against potent free radical reactions. *Clin Biochem* 37: 112–119, 2004.

16. **Erel O**. A new automated colorimetric method for measuring total oxidant status. *Clin Biochem* 38: 1103–1111, 2005.

17. **Fonović M**, **Turk B**. Cysteine cathepsins and extracellular matrix degradation. *Biochim Biophys Acta* 1840: 2560–2570, 2014.

18. **Foronjy RF**, **Dabo AJ**, **Taggart CC**, **Weldon S**, **Geraghty P**. Respiratory syncytial virus infections enhance cigarette smoke induced COPD in mice. *PloS One* 9: e90567, 2014.

19. **Geraghty P**, **Greene CM**, **O'Mahony M**, **O'Neill SJ**, **Taggart CC**, **McElvaney NG**. Secretory leucocyte protease inhibitor inhibits interferon-gamma-induced cathepsin S expression. *J Biol Chem* 282: 33389–33395, 2007.

20. **Geraghty P**, **Rogan MP**, **Greene CM**, **Brantly ML**, **O'Neill SJ**, **Taggart CC**, **McElvaney NG**. Alpha-1-antitrypsin aerosolised augmentation abrogates neutrophil elastase-induced expression of cathepsin B and matrix metalloprotease 2 in vivo and in vitro. *Thorax* 63: 621–626, 2008.

21. **Giles NM**, **Watts AB**, **Giles GI**, **Fry FH**, **Littlechild JA**, **Jacob C**. Metal and redox modulation of cysteine protein function. *Chem Biol* 10: 677–693, 2003.

22. **Golovatch P**, **Mercer BA**, **Lemaître V**, **Wallace A**, **Foronjy RF**, **D'Armiento J**. Role for cathepsin K in emphysema in smoke-exposed guinea pigs. *Exp Lung Res* 35: 631–645, 2009.

23. **de Groot LES**, **van der Veen TA**, **Martinez FO**, **Hamann J**, **Lutter R**, **Melgert BN**. Oxidative stress and macrophages: driving forces behind exacerbations of asthma and chronic obstructive pulmonary disease? *Am J Physiol Lung Cell Mol Physiol* 316: L369–L384, 2019.

24. **Gueugnon F**, **Barascu A**, **Mavridis K**, **Petit-Courty A**, **Marchand-Adam S**, **Gissot V**, **Scorilas A**, **Guyetant S**, **Courty Y**. Kallikrein-related peptidase 13: an independent indicator of favorable prognosis for patients with nonsmall cell lung cancer. *Tumor Biol* 36: 4979–4986, 2015.

25. **Hogg JC**. Pathophysiology of airflow limitation in chronic obstructive pulmonary disease. *Lancet Lond Engl* 364: 709–721, 2004.

26. **Hukkanen J**, **Pelkonen O**, **Hakkola J**, **Raunio H**. Expression and regulation of xenobiotic-metabolizing cytochrome P450 (CYP) enzymes in human lung. *Crit Rev Toxicol* 32: 391–411, 2002.

27. **Jha P**, **Ramasundarahettige C**, **Landsman V**, **Rostron B**, **Thun M**, **Anderson RN**, **McAfee T**, **Peto R**. 21st-century hazards of smoking and benefits of cessation in the United States. *N Engl J Med* 368: 341–350, 2013.

28. **Kang M-J**, **Homer RJ**, **Gallo A**, **Lee CG**, **Crothers KA**, **Cho SJ**, **Rochester C**, **Cain H**, **Chupp G**, **Yoon HJ**, **Elias JA**. IL-18 is induced and IL-18 receptor alpha plays a critical role in the pathogenesis of cigarette smoke-induced pulmonary emphysema and inflammation. *J Immunol* 178: 1948–1959, 2007.

29. **Kehlet SN**, **Bager CL**, **Willumsen N**, **Dasgupta B**, **Brodmerkel C**, **Curran M**, **Brix S**, **Leeming DJ**, **Karsdal MA**. Cathepsin-S degraded decorin are elevated in fibrotic lung disorders - development and biological validation of a new serum biomarker. *BMC Pulm Med* 17: 110, 2017.

30. **Kos J**, **Sekirnik A**, **Kopitar G**, **Cimerman N**, **Kayser K**, **Stremmer A**, **Fiehn W**, **Werle B**. Cathepsin S in tumours, regional lymph nodes and sera of patients with lung cancer: relation to prognosis. *Br J Cancer* 85: 1193–1200, 2001.

31. **Kramer L**, **Turk D**, **Turk B**. The Future of Cysteine Cathepsins in Disease Management. *Trends Pharmacol Sci* 38: 873–898, 2017.

32. **Lalmanach G**, **Saidi A**, **Marchand-Adam S**, **Lecaille F**, **Kasabova M**. Cysteine cathepsins and cystatins: from ancillary tasks to prominent status in lung diseases. *Biol Chem* 396: 111–130, 2015.

33. **Lecaille F**, **Lalmanach G**, **Andrault P-M**. Antimicrobial proteins and peptides in human lung diseases: A friend and foe partnership with host proteases. *Biochimie* 122: 151–168, 2016.

34. **Lommatzsch M**, **Cicko S**, **Müller T**, **Lucattelli M**, **Bratke K**, **Stoll P**, **Grimm M**, **Dürk T**, **Zissel G**, **Ferrari D**, **Di Virgilio F**, **Sorichter S**, **Lungarella G**, **Virchow JC**, **Idzko M**. Extracellular adenosine triphosphate and chronic obstructive pulmonary disease. *Am J Respir Crit Care Med* 181: 928–934, 2010.

35. **Lopez-Castejon G**, **Theaker J**, **Pelegrin P**, **Clifton AD**, **Braddock M**, **Surprenant A**. P2X(7) receptor-mediated release of cathepsins from macrophages is a cytokine-independent mechanism potentially involved in joint diseases. *J Immunol* 185: 2611–2619, 2010.

36. **Lu Q**, **Gottlieb E**, **Rounds S**. Effects of cigarette smoke on pulmonary endothelial cells. *Am J Physiol Lung Cell Mol Physiol* 314: L743–L756, 2018.

37. **Lucattelli M**, **Cicko S**, **Müller T**, **Lommatzsch M**, **De Cunto G**, **Cardini S**, **Sundas W**, **Grimm M**, **Zeiser R**, **Dürk T**, **Zissel G**, **Sorichter S**, **Ferrari D**, **Di Virgilio F**, **Virchow JC**, **Lungarella G**, **Idzko M**. P2X7 receptor signaling in the pathogenesis of smoke-induced lung inflammation and emphysema. *Am J Respir Cell Mol Biol* 44: 423–429, 2011.

38. **Mallia-Milanes B**, **Dufour A**, **Philp C**, **Solis N**, **Klein T**, **Fischer M**, **Bolton CE**, **Shapiro S**, **Overall CM**, **Johnson SR**. TAILS proteomics reveals dynamic changes in airway proteolysis controlling protease activity and innate immunity during COPD exacerbations. *Am J Physiol Lung Cell Mol Physiol* 315: L1003–L1014, 2018.

39. **McMaster SK**, **Paul-Clark MJ**, **Walters M**, **Fleet M**, **Anandarajah J**, **Sriskandan S**, **Mitchell JA**. Cigarette smoke inhibits macrophage sensing of Gram-negative bacteria and lipopolysaccharide: relative roles of nicotine and oxidant stress. *Br J Pharmacol* 153: 536–543, 2008.

40. **Motz GT**, **Eppert BL**, **Wesselkamper SC**, **Flury JL**, **Borchers MT**. Chronic cigarette smoke exposure generates pathogenic T cells capable of driving COPD-like disease in Rag2-/- mice. *Am J Respir Crit Care Med* 181: 1223–1233, 2010.

41. **Nakajima T**, **Nakamura H**, **Owen CA**, **Yoshida S**, **Tsuduki K**, **Chubachi S**, **Shirahata T**, **Mashimo S**, **Nakamura M**, **Takahashi S**, **Minematsu N**, **Tateno H**, **Fujishima S**, **Asano K**, **Celli BR**, **Betsuyaku T**. Plasma Cathepsin S and Cathepsin S/Cystatin C Ratios Are Potential Biomarkers for COPD. *Dis Markers* 2016: 4093870, 2016.

42. **Naudin C**, **Joulin-Giet A**, **Couetdic G**, **Plésiat P**, **Szymanska A**, **Gorna E**, **Gauthier F**, **Kasprzykowski F**, **Lecaille F**, **Lalmanach G**. Human Cysteine Cathepsins Are Not Reliable Markers of Infection by Pseudomonas aeruginosa in Cystic Fibrosis. *PLoS One* 6: e25577, 2011.

43. **Reiser J**, **Adair B**, **Reinheckel T**. Specialized roles for cysteine cathepsins in health and disease. *J Clin Invest* 120: 3421–3431, 2010.

44. **Rovina N**, **Dima E**, **Gerassimou C**, **Kollintza A**, **Gratziou C**, **Roussos C**. Interleukin-18 in induced sputum: association with lung function in chronic obstructive pulmonary disease. *Respir Med* 103: 1056–1062, 2009.

45. **Russell REK**, **Culpitt SV**, **DeMatos C**, **Donnelly L**, **Smith M**, **Wiggins J**, **Barnes PJ**. Release and activity of matrix metalloproteinase-9 and tissue inhibitor of metalloproteinase-1 by alveolar macrophages from patients with chronic obstructive pulmonary disease. *Am J Respir Cell Mol Biol* 26: 602–609, 2002.

46. **Sage J**, **Leblanc-Noblesse E**, **Nizard C**, **Sasaki T**, **Schnebert S**, **Perrier E**, **Kurfurst R**, **Brömme D**, **Lalmanach G**, **Lecaille F**. Cleavage of nidogen-1 by cathepsin S impairs its binding to basement membrane partners. *PloS One* 7: e43494, 2012.

47. **Schamberger AC**, **Mise N**, **Jia J**, **Genoyer E**, **Yildirim AÖ**, **Meiners S**, **Eickelberg O**. Cigarette smoke-induced disruption of bronchial epithelial tight junctions is prevented by transforming growth factor-β. *Am J Respir Cell Mol Biol* 50: 1040–1052, 2014.

48. **Schamberger AC**, **Schiller HB**, **Fernandez IE**, **Sterclova M**, **Heinzelmann K**, **Hennen E**, **Hatz R**, **Behr J**, **Vašáková M**, **Mann M**, **Eickelberg O**, **Staab-Weijnitz CA**. Glutathione peroxidase 3 localizes to the epithelial lining fluid and the extracellular matrix in interstitial lung disease. *Sci Rep* 6: 29952, 2016.

49. **Schwarz G**, **Boehncke W-H**, **Braun M**, **Schröter CJ**, **Burster T**, **Flad T**, **Dressel D**, **Weber E**, **Schmid H**, **Kalbacher H**. Cathepsin S activity is detectable in human keratinocytes and is selectively upregulated upon stimulation with interferon-gamma. *J Invest Dermatol* 119: 44–49, 2002.

50. **Shi GP**, **Munger JS**, **Meara JP**, **Rich DH**, **Chapman HA**. Molecular cloning and expression of human alveolar macrophage cathepsin S, an elastinolytic cysteine protease. *J Biol Chem* 267: 7258–7262, 1992.

51. **Staab-Weijnitz CA**, **Fernandez IE**, **Knüppel L**, **Maul J**, **Heinzelmann K**, **Juan-Guardela BM**, **Hennen E**, **Preissler G**, **Winter H**, **Neurohr C**, **Hatz R**, **Lindner M**, **Behr J**, **Kaminski N**, **Eickelberg O**. FK506-Binding Protein 10, a Potential Novel Drug Target for Idiopathic Pulmonary Fibrosis. *Am J Respir Crit Care Med* 192: 455–467, 2015.

52. **Storm van's Gravesande K**, **Layne MD**, **Ye Q**, **Le L**, **Baron RM**, **Perrella MA**, **Santambrogio L**, **Silverman ES**, **Riese RJ**. IFN regulatory factor-1 regulates IFN-gamma-dependent cathepsin S expression. *J Immunol* 168: 4488–4494, 2002.

53. **Taggart C**, **Mall MA**, **Lalmanach G**, **Cataldo D**, **Ludwig A**, **Janciauskiene S**, **Heath N**, **Meiners S**, **Overall CM**, **Schultz C**, **Turk B**, **Borensztajn KS**. Protean proteases: at the cutting edge of lung diseases. *Eur Respir J* 49, 2017.

54. **Vasiljeva O**, **Reinheckel T**, **Peters C**, **Turk D**, **Turk V**, **Turk B**. Emerging roles of cysteine cathepsins in disease and their potential as drug targets. *Curr Pharm Des* 13: 387–403, 2007.

55. **Wang Z**, **Zheng T**, **Zhu Z**, **Homer RJ**, **Riese RJ**, **Chapman HA**, **Shapiro SD**, **Elias JA**. Interferon gamma induction of pulmonary emphysema in the adult murine lung. *J Exp Med* 192: 1587–1600, 2000.

56. **Weldon S**, **McNally P**, **McAuley DF**, **Oglesby IK**, **Wohlford-Lenane CL**, **Bartlett JA**, **Scott CJ**, **McElvaney NG**, **Greene CM**, **McCray PB**, **Taggart CC**. *Am J Respir Crit Care Med* 190: 165–174, 2014.

57. **Wilkinson RDA**, **Williams R**, **Scott CJ**, **Burden RE**. Cathepsin S: therapeutic, diagnostic, and prognostic potential. *Biol Chem* 396: 867–882, 2015.

58. **Williams AS**, **Eynott PR**, **Leung S-Y**, **Nath P**, **Jupp R**, **De Sanctis GT**, **Resnick R**, **Adcock IM**, **Chung KF**. Role of cathepsin S in ozone-induced airway hyperresponsiveness and inflammation. *Pulm Pharmacol Ther* 22: 27–32, 2009.

59. **Wu J**, **Sin DD**. Improved patient outcome with smoking cessation: when is it too late? *Int J Chron Obstruct Pulmon Dis* 6: 259–267, 2011.

60. **Zheng T**, **Kang MJ**, **Crothers K**, **Zhu Z**, **Liu W**, **Lee CG**, **Rabach LA**, **Chapman HA**, **Homer RJ**, **Aldous D**, **De Sanctis GT**, **Desanctis G**, **Underwood S**, **Graupe M**, **Flavell RA**, **Schmidt JA**, **Elias JA**. Role of cathepsin S-dependent epithelial cell apoptosis in IFN-gamma-induced alveolar remodeling and pulmonary emphysema. *J Immunol Baltim Md 1950* 174: 8106–8115, 2005.

61. **Zheng T**, **Zhu Z**, **Wang Z**, **Homer RJ**, **Ma B**, **Riese RJ**, **Chapman HA**, **Shapiro SD**, **Elias JA**. Inducible targeting of IL-13 to the adult lung causes matrix metalloproteinase- and cathepsin-dependent emphysema. *J Clin Invest* 106: 1081–1093, 2000.

857 62. **Zhong C-Y**, **Zhou Y-M**, **Douglas GC**, **Witschi H**, **Pinkerton KE**. MAPK/AP-1 signal
858 pathway in tobacco smoke-induced cell proliferation and squamous metaplasia in the
859 lungs of rats. *Carcinogenesis* 26: 2187–2195, 2005.

860 63. WHO report on the global tobacco epidemic 2017 [Online]. [date unknown].
861 http://www.who.int/tobacco/global_report/en/ [10 Oct. 2018].

862

863 **Table 1: Patient characteristics**

	non-COPD			COPD					
				GOLD I		GOLD II		GOLD III	
Smoking status	NS	CS	FS	CS	FS	CS	FS	CS	FS
No. of subjects	10	10	10	7	10	9	9	2	5
Sex, M/F	2/8	9/1	9/1	5/2	9/1	6/3	9/0	2/0	5/0
Age, years (SD)	73(7)	54*(11)	62(9)	62(6)	66(12)	60(9)	63(8)	61(10)	68(5)
Pack-years (SD)	0	28(13)	40(15)	54(26)	32(15)	64(26)	54(24)	49(24)	55(13)
FEV_1, % predicted (SD)	99(19)	92(19)	83(11)	92(6)	99(14)	69*(9)	69*(8)	34*(3)	43*(3)

864

865 Smoking status is noted as: NS, never-smoker; CS, current smoker; FS, former smoker. Data
866 are presented as n or mean with standard deviation (SD), unless otherwise stated. FEV1: forced
867 expiratory volume in one second. Mean age of each group was compared using Kruskal-Wallis
868 test (*: $p<0.05$ compared with NS). FEV_1 data were compared using Kruskal-Wallis test (*:
869 $p<0.05$ *versus* non-COPD (NS, CS and FS) patients and GOLD I (CS, FS) patients).

870

Table 2: Median levels of TAS, TOS and OSI in never-smokers, non-COPD and COPD current smokers

	NS (n=10)	Non-COPD CS (n=10)	COPD CS (n=18)
TAS (mM Trolox eq./µg protein)	529(149)	373*(112)	385*(123)
TOS (µM H_2O_2 eq./ µg protein)	314(40)	355*(60)	362*(186)
OSI	0.59(0.1)	0.95****(0.1)	0.94****(0.2)

TAS: Total Antioxidant Status, TOS: Total Oxidant Status, OSI Oxidative Stress Index. Results are expressed as median with standard deviation (SD). Data from non-COPD CS and COPD CS were compared with NS, using Mann-Whitney U test (*: $p<0.05$; ****: $p<0.0001$).

884 **Legends to Figures**

885

886 **Figure 1: Cathepsin S protein expression in peripheral lung tissue of never-smokers and**
887 **smokers.**

888 A) Lung tissue was obtained from never-smokers (NS), non-COPD current smokers (CS) and
889 CS with COPD. Representative histological sections (original magnification: 400 x) of
890 bronchiolar and alveolar epithelium are shown to illustrate the difference between NS, non-
891 COPD CS (*middle*) and COPD CS (Gold III) (*right*) (*Bars*, 100 µm). The lung parenchyma
892 and elastin fibers were respectively stained with hematoxylin-phloxine-saffron (HPS) and
893 orcein. Elastin fibers are highlighted with arrows. Expression of CatS was visualized by
894 immunohistochemistry (IHC) using primary antibody against CatS (1:100) and an anti-CD68
895 antibody (1:200) was used to highlight the alveolar macrophages. B) Representative Western-
896 blot of mature CatS in peripheral lung tissue lysates (30 µg/well) of five NS, five non-COPD
897 CS and five CS with COPD. Patient ID numbers are shown on top. C) Total CatS expression
898 was evaluated by ELISA in lung tissue lysates from NS patients (n=10) and smokers (n=62,
899 including non-COPD CS, FS, and COPD CS, FS) and the concentration (pg/mL) normalised
900 to total tissue homogenate protein content (pg/µg of total protein). Bars represent mean
901 values±SD. Statistical significance was assessed using Mann-Whitney *U* test (*: $p<0.05$).

902

903 **Figure 2: Cathepsin S protein levels are higher in current smokers with or without**
904 **COPD.**

905 A) Total CatS levels in tissue lysates from never-smokers (NS) and smokers with different
906 status including current smokers (CS), former smokers (FS) w/o COPD, and CS and FS with
907 COPD (Gold I-III) were quantified by ELISA. Statistical significance was assessed using
908 Kruskal-Wallis test (Dunn's multiple comparisons) (*: $p<0.05$; **: $p<0.01$). B) Correlation
909 between CatS levels and smoking history (packs/year), and C) the lung function evaluated as
910 forced expiratory volume in 1 s (FEV_1) in samples from NS and CS (non-COPD and COPD).
911 Correlations were determined by linear regression and indicated by the Spearman coefficient
912 (r_s) and levels of significance (p). D) Correlation between the lung function evaluated as
913 forced expiratory volume in 1 s (FEV_1, % predicted) and smoking history (packs/year).
914 Correlation was determined by linear regression and indicated by the Spearman coefficient
915 (r_s) and levels of significance (p). E) Representative Western-blot of CatS expression (white
916 arrow: proform, black arrow: mature form) in tissue lysates from different groups; NS, non-
917 COPD CS and FS, CS and FS with different stages of COPD severity (GOLD I, mild; GOLD

II, moderate; GOLD III, severe, total protein amount: 30 µg of protein pooled from equal amount of samples from each group). β-actin normalized densitometric analysis of mature CatS immunoreactive bands was performed using the ImageJ softwareand data are represented as mean±SD. G) Total CatS levels in tissue lysate from NS and CS with COPD and H) from NS and FS with COPD were quantified by ELISA. Concentration of CatS assessed by ELISA (pg/mL) were normalised to total tissue homogenate protein content (pg/µg of total protein). Statistical analyses of CatS levels were performed for each category of smokers using Mann-Whitney *U* test and values were compared with NS (*: $p<0.05$).

Figure 3: Cathepsin S activity is higher in lung tissue lysates of current smokers.

A) Titration of active CatS in tissue lysates. Detection of active-site titration of CatS in tissue lysate (10 µg of total protein) of each patient. Titration was performed with E-64 (0-20 nM) before adding Z-Leu-Arg-AMC (50 µM). B) Titration of CatS in tissue lysates from never-smokers (NS) and current smokers (CS) with COPD and C) from NS and former smokers (FS) with COPD. Values were normalized to the respective loading control and data are represented as mean±SD. Statistical analyses of CatS activity were performed using Kruskal-Wallis test (Dunn's multiple comparisons) (*: $p<0.05$; **: $p<0.01$). D) Elastinolytic activity of CatS in tissue lysates from NS and all smokers, using DQ-elastin as a substrate. Controls were performed using the CatS inhibitor (LHVS, 100 nM). Statistical analyses of CatS activity were performed using Mann−Whitney *U* test (***: $p<0.001$). E) Correlation between active site titration of CatS and smoking history (packs/year), and F) FEV_1 (% predicted) in samples from NS and CS (non-COPD and COPD). Correlations were determined by linear regression and indicated by the Spearman coefficient (r_s) and levels of significance (p).

Figure 4: Effects of cigarette smoke extract (CSE) on pHBECs viability and mitochondrial oxidative stress induction.

A) LDH assay performed with confluent pHBECs treated with 0 to 50% CSE for 2 and 24 h. Data were normalized to time-matched controls and represent mean ± SD of three independent experiments. B) Cell morphology of pHBECs treated with indicated concentrations of CSE for 2 and 24 h. Representative bright field images are shown (original magnification: x100; insets: x200). C) Quantification of MitoSOX by flow cytometry. Cells were treated for 2 h with CSE (0%, 2.5%, 5%, 10%, and 20%). Data were normalized to control (dashed lane) and represent mean ± SD of three independent experiments. For statistical analysis, Kruskal-Wallis test was used (*: $p<0.05$; **: $p<0.01$ *vs* control).

Figure 5: Effects of cigarette smoke extract (CSE) on cathepsin S expression in pHBECs.

Cultures of pHBECs were treated with 0%, 2.5%, 5%, 10%, or 20% cigarette smoke extract (CSE) for 2 h. A) Representative Western-blot of CatS in pHBECs whole-cell lysates (total protein amount: 5 µg/ lane) using an anti-CatS polyclonal antibody. Anti-β-actin polyclonal antibody was used as a loading control. B) Protein levels of CatS were determined by ELISA. Bars represent mean values ± SD from three independent pHBEC donors (duplicate). Statistical analyses of CatS levels were performed for each dose of CSE using Mann-Whitney *U* test and values were compared to control (*: $p<0.05$). C) Total cathepsin activity in whole-cell lysates of pHBECs (total protein amount: 100 ng) was measured using Z-Phe-Arg-AMC (50 µM) in 100 mM sodium acetate buffer, pH 5.5, 5 mM DTT, and 0.01% Brij35. D) Western-blot analysis of LL-37 hydrolysis by pHBEC cell free lysates (treated or not with 10 % CSE) for 0-24 h. Controls were performed with E-64 and LHVS. Representative blot using an anti-LL-37 antibody is shown. E) Representative Western-blot of CatS (upper panel) in whole-cell lysates of pHBECs (total protein amount: 5 µg/ lane) exposed or not to CSE for 2 h (2.5%). Cells were pre-treated 1 h with P2X7 receptor antagonist (1 µM), or mock (DMSO). Respective CatS densitometry (lower panel). Statistical analyses were performed using Mann-Whitney *U* test (*: $p<0.05$). F) Representative Western-blot showing expression of phosphorylated-p38 MAPK (Thr180/Tyr182) and phosphorylated-cPLA$_2$ (Ser505) in CSE-exposed pHBECs.

Figure 6: **Proposed mechanism of the induction of cathepsin S expression by cigarette smoke exposure of pHBECs.**

Schematic overview of the existing literature on cigarette smoke exposure causes an increase in ATP from primary human bronchial epithelial cells, via the activation of TRPV1, TRPV4 and pannexin-1 channels (5). ATP activates P2X7 receptors leading to efflux of K^+ and influx of Ca^{2+} (13). Increase of cytosolic Ca^{2+} levels stimulate p38 MAPK phosphorylation leading to an increase of phospholipase A_2 (cPLA$_2$) expression, leading to the release of lysosomal CatS. In bold are depicted the results of the present study.

Figure 7: Effect of cigarette smoke extract (CSE) on cathepsin S activity.

A) CSE preparation was standardized by measuring the absorbance at 320 nm at pH 5.5 (filled black diamond) and 7.4 (empty circle). B) The oxidant potential of each CSE

preparation was measured by its ability to convert non-fluorescent dihydrorhodamine-123 to oxidized fluorescent rhodamine-123 (λ_{exc}: 490 nm, λ_{em}: 530 nm) at pH 5.5 (filled black diamond) and 7.4 (empty circle). C) Inhibition of CatS activity by CSE. CatS (1 nM) activity (relative fluorescence unit, RFU) was measured continuously (0-60 min) at 37°C in the presence or absence of CSE (2.5-40 %) at pH 5.5 and 7.4, using Z-Leu-Arg-AMC (20 μM) as a substrate. D) CatS (1 nM) was preincubated at 37°C for 10 min in the presence or absence of CSE (2.5-40 %) at pH 5.5 (filled black diamond) and 7.4 (empty circle), and residual activity was monitored at 37°C using Z-Leu-Arg-AMC (20 μM).

Figure 1

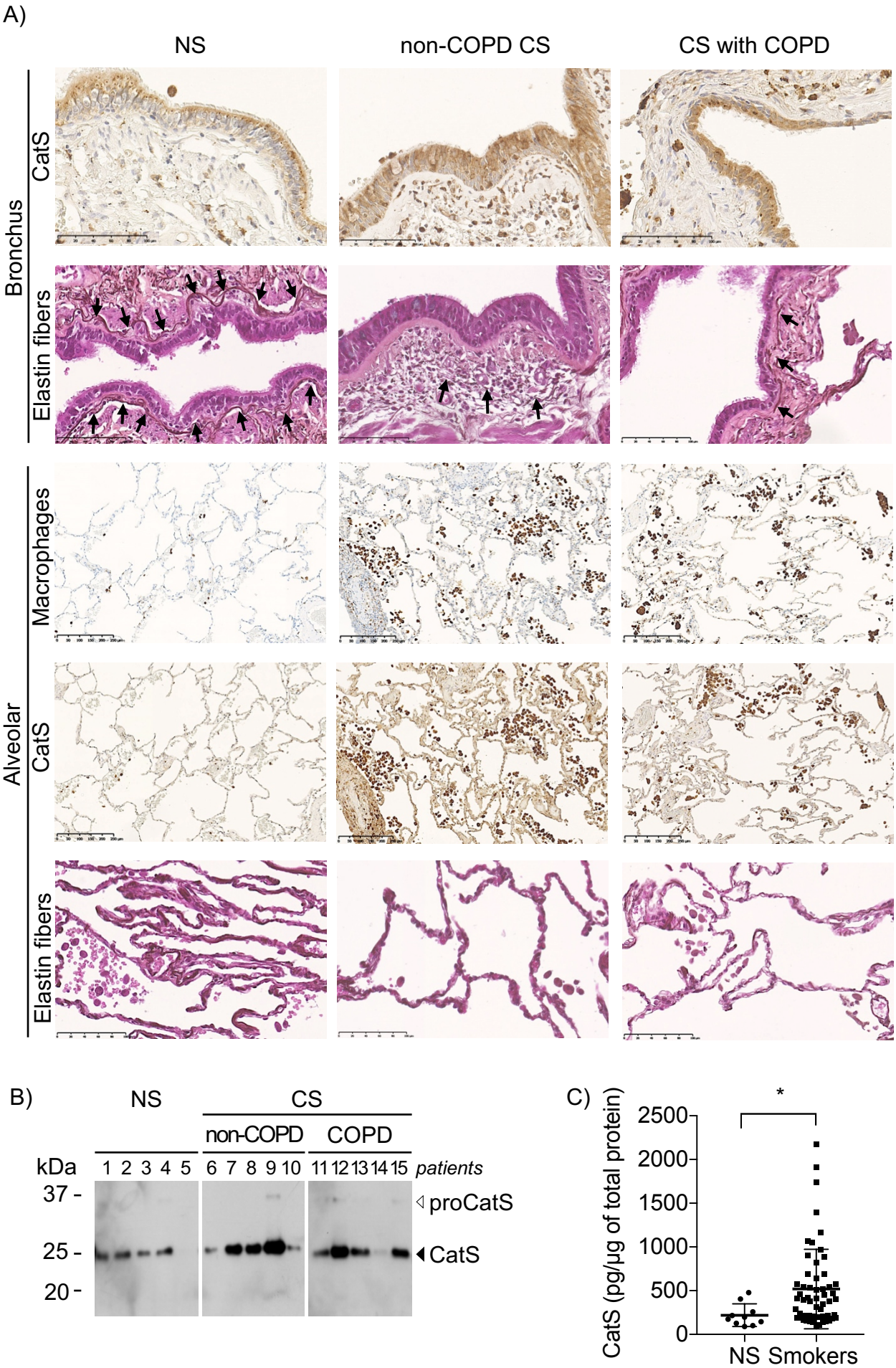

Figure 2

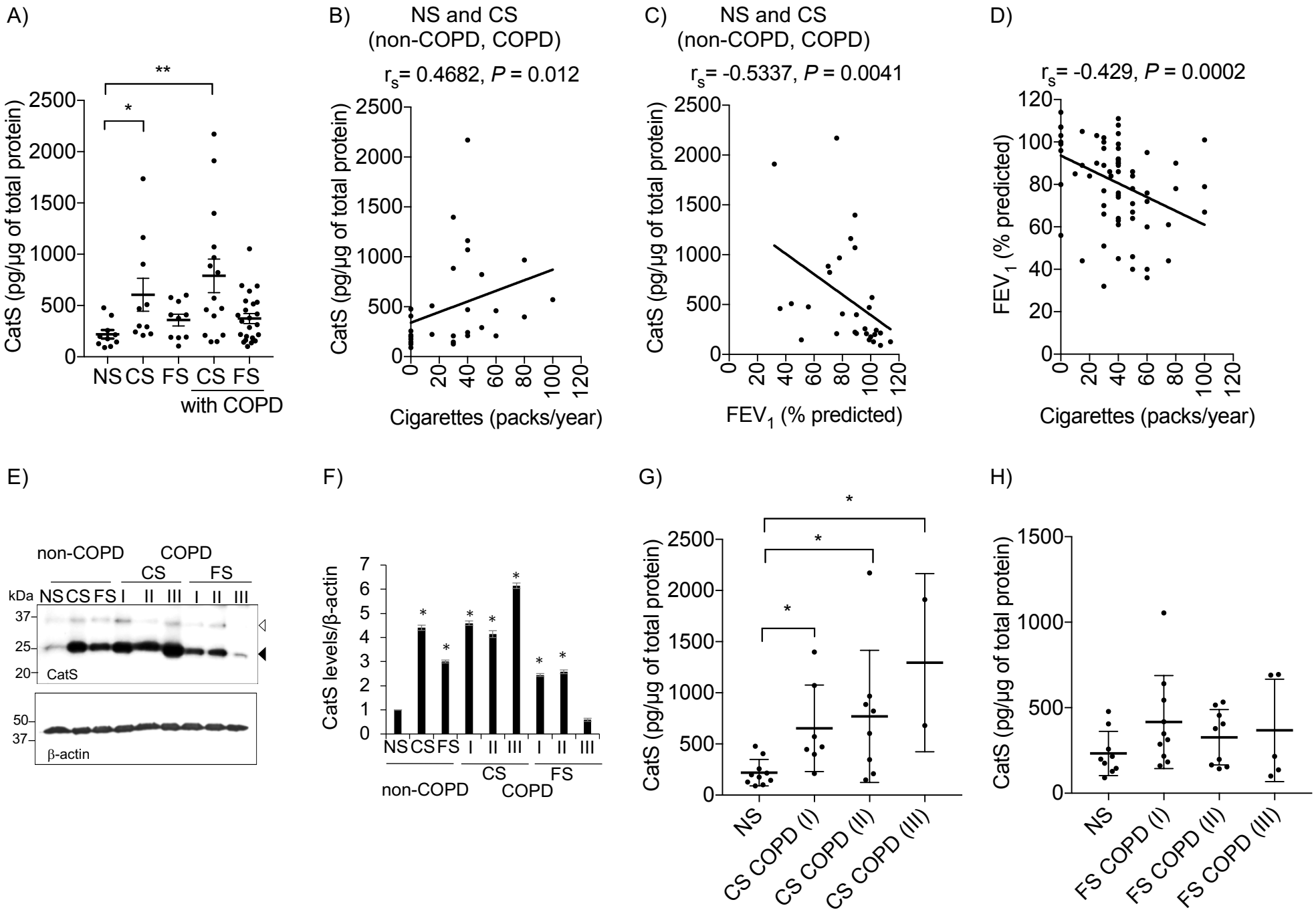

Figure 3

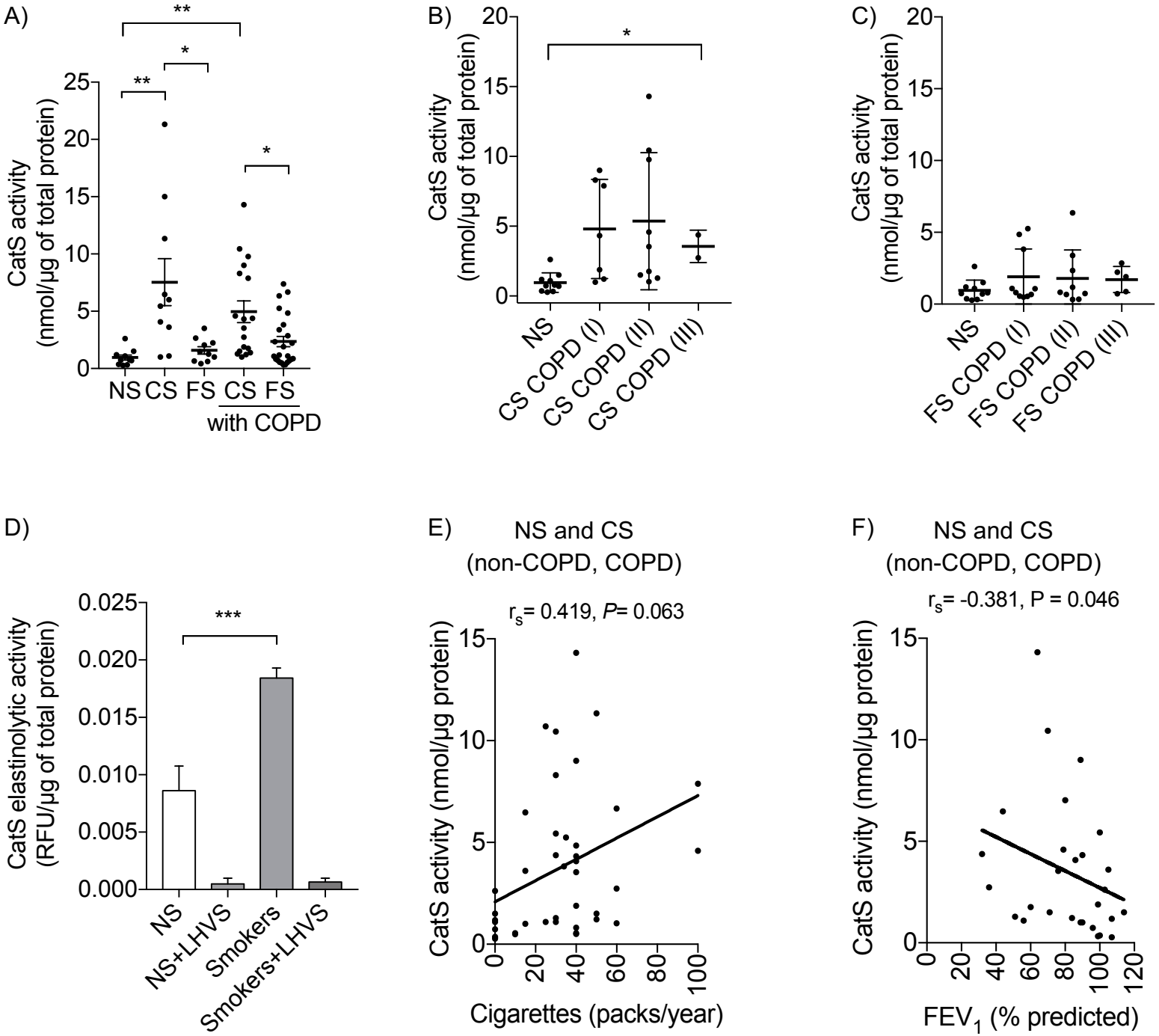

Figure 4

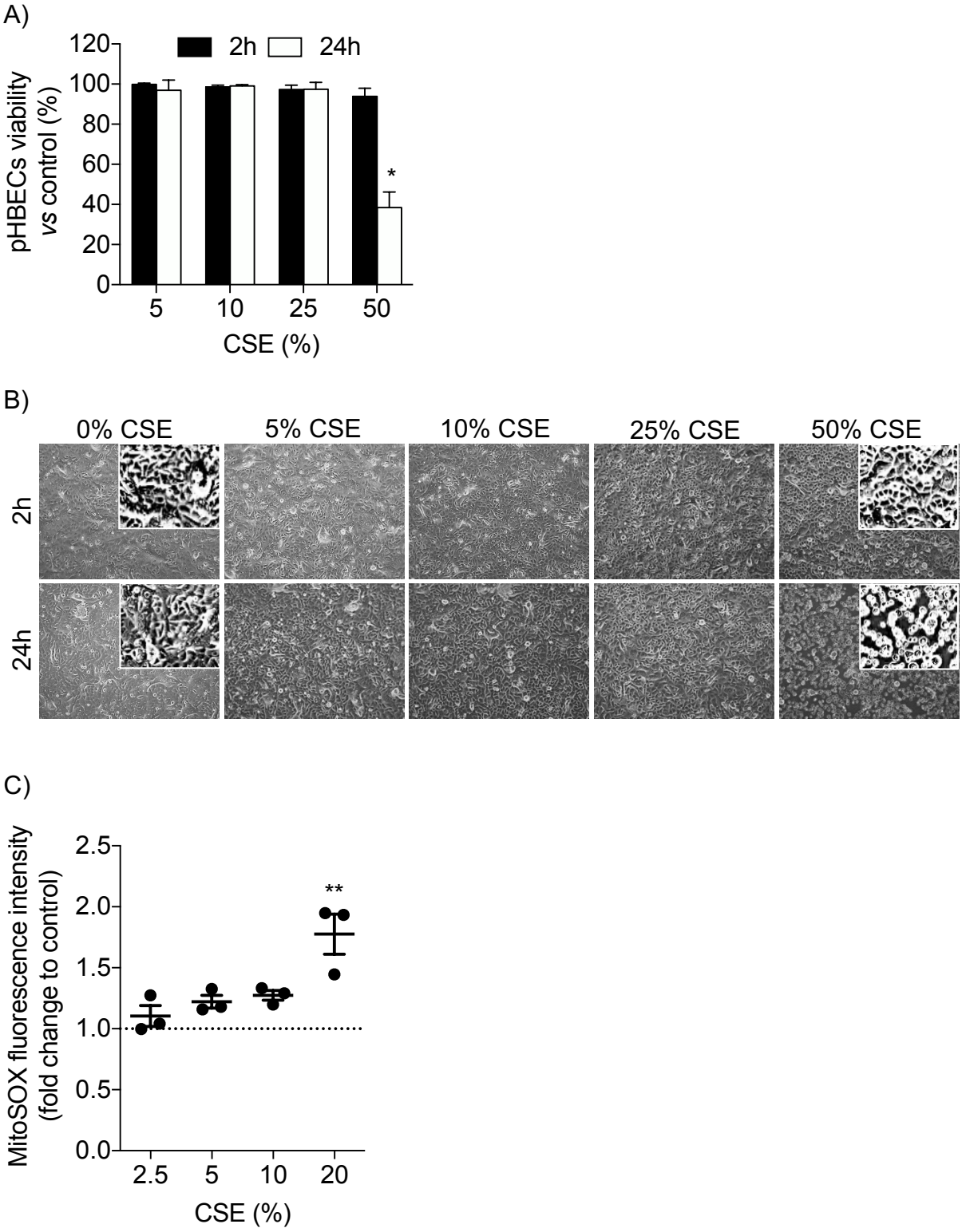

Figure 5

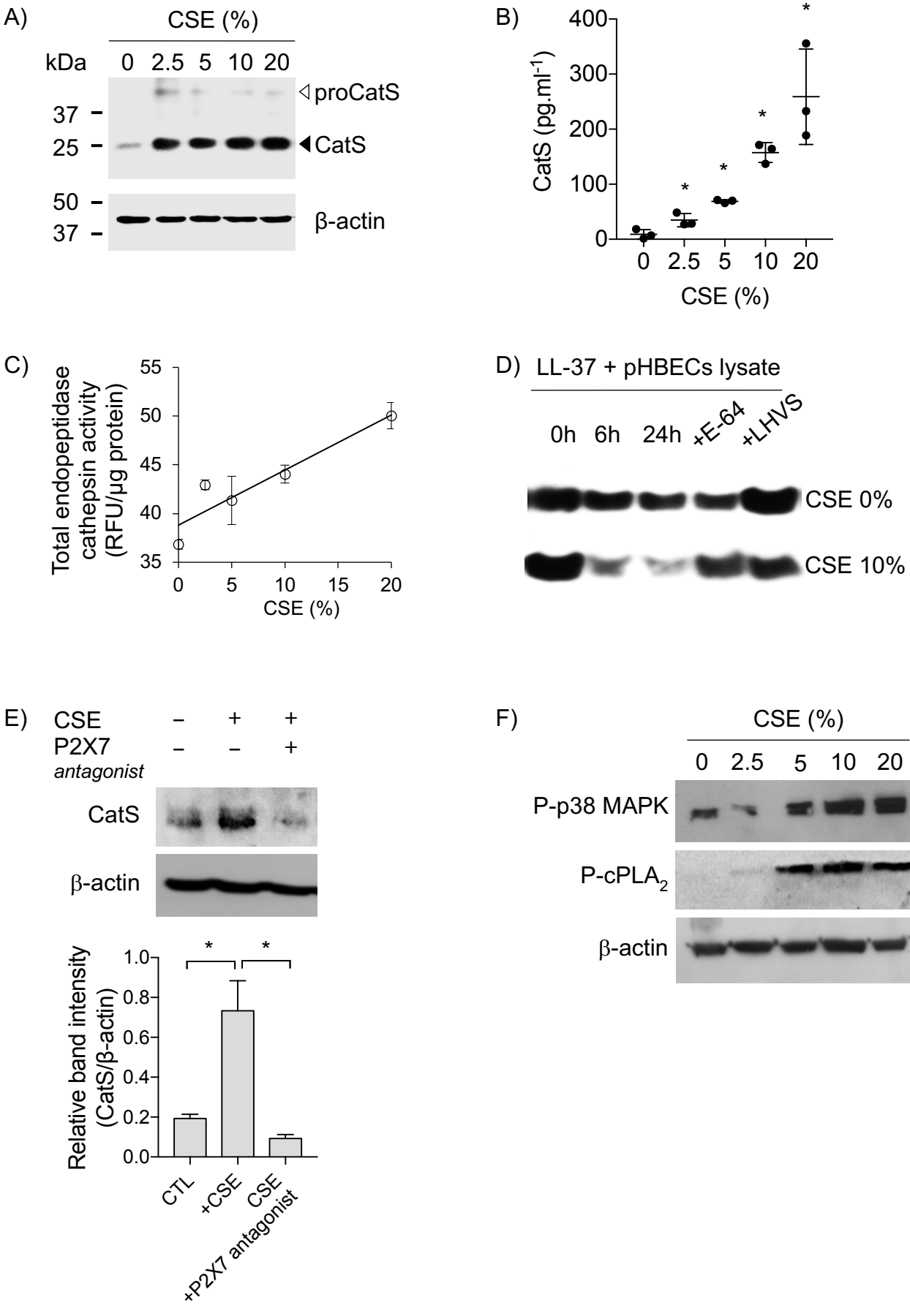

Figure 6

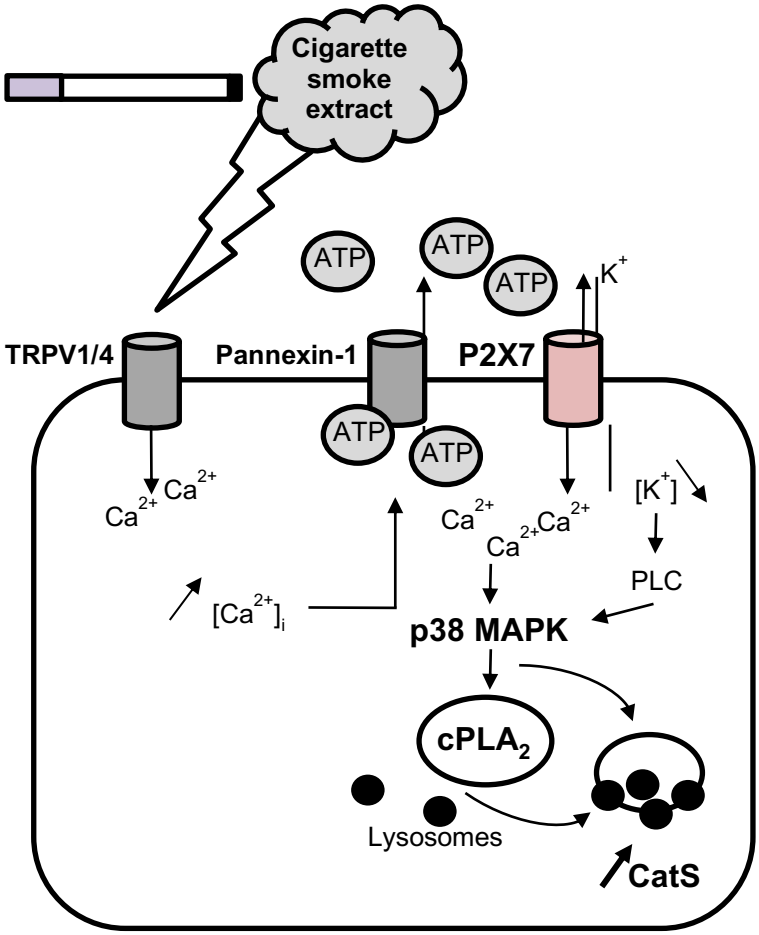

Figure 7